Krafft temperature and enthalpy of solution of N-acyl amino acid surfactants and their racemic modifications: Effect of the amino acid residue

Colloid Polymer Sci. 2002 in press

Krafft Temperature and Enthalpy of Solution of *N*-Acyl Amino Acid Surfactants and Their Racemic Modifications: Effect of the Amino Acid Residue

Akio Ohta, Noriaki Ozawa, Satoru Nakashima, Tsuyoshi Asakawa, and Shigeyoshi Miyagishi

Department of Chemistry and Chemical Engineering, Faculty of Engineering, Kanazawa University, Ishikawa 920-8667, Japan

Mailing address:
Akio Ohta
Department of Chemistry and Chemical Engineering, Faculty of Engineering, Kanazawa University, 2-40-20 Kodatsuno, Kanazawa, Ishikawa 920-8667, Japan

e-mail address
akio-o@t.kanazawa-u.ac.jp

1. To whom the correspondence should be addressed.

Abstract

The Krafft temperatures and the enthalpies of solution of six kinds of *N*-hexadecanoyl amino acid surfactant (Gly, Ala, Val, Leu, Ile, and Phe) were obtained from both solubility measurements and differential scanning calorimetry. It was shown that the Krafft temperature of *N*-hexadecanoyl amino acid surfactant increased with decreasing size of the amino acid residue except for the case of phenylalanine. On the other hand, the enthalpy of solution was endothermic and increased with decreasing size of the amino acid residue except for the cases of glycine and phenylalanine. It was found from these results that the D-L interaction was superior to the L-L interaction in solid state of *N*-hexadecanoyl amino acid surfactant salt for both the alanine and phenylalanine systems. It was suggested by *ab initio* calculations that the difference of the magnitude of the peptide-peptide hydrogen bonding was dominant factor for the chiral effect.

Keywords *N*-Acyl amino acid surfactant • Krafft temperature • Enthalpy of solution • Amino acid residue • Chiral effect

Introduction

N-Acyl amino acid surfactants, which are anionic amino acid-type surfactants, are of immense importance both from the industrial and the domestic viewpoints because of their biodegradability and low toxicity [1]. Micelle formation is an important property of surfactants, and has been the subject of intense research [2-8]. The aggregation number of a micelle is same order as that for general anionic surfactants (ca. 40~100) and

increases with increasing concentrations of surfactant and/or salt [4,5,8]. Furthermore *N*-acyl amino acid surfactants are useful for chiral discrimination. There are two types of chiral discrimination; one in which the D-L interaction is more favorable, and a second where the D-D or L-L interaction is more favorable. The latter is especially important from the standpoint of improving optical purity. The chiral discrimination of *N*-acyl amino acid surfactants has been reported in the solid state [9,10], Langmuir monolayer [11-15], and even for micelles [2,16]. This effect in the expanded state of a Langmuir monolayer and micelle, however, is much smaller than in the solid and condensed state of a Langmuir monolayer. However, the ability of *N*-acyl amino acid surfactants to act as chiral selectors have been confirmed for both micelles [17-19] and copper complexes [20,21]. Therefore, these compounds have enormous potential as column packing material for chiral chromatography.

In this study, the effects of the size of the hydrophobic residue of *N*-hexadecanoyl amino acid surfactants on the Krafft temperature (KT) and the enthalpy of solution are investigated by both solubility measurements and differential scanning calorimetry (DSC). It is known that the KT is an important property of a surfactant because micelle particles appear in aqueous solution only above the KT. This has obvious applications in industrial processes where the KT is critical then it is also important to investigate the effect of the amino acid residue on the KT of *N*-Acyl amino acid surfactants. In addition, we also studied the chiral effects of *N*-hexadecanoyl amino acid surfactant on the KT and the enthalpy of solution. These are discussed from the viewpoint of homochiral (L-L or D-D) and the heterochiral (D-L) interactions by use of theoretical calculations.

Experimental

Materials

Glycine (Gly), L-alanine (Ala), L-valine (Val), L-leucine (Leu), L-isoleucine (Ile), L-phenylalanine (Phe) and their racemic mixtures (DL-form) were purchased from Peptide Institute, Inc. and Nacalai Tesque, Inc., and used without further purification. *N*-Hexadecanoyl amino acids (C16-amino acid; see Fig.1) were synthesized by the reaction of an amino acid with hexadecanoyl chloride as described previously [2] and were re-crystallized from mixtures of either diethyl ether-ethanol or acetone-methanol. Their purities were checked by HPLC and DSC and by observing no minimum on the surface tension vs concentration curves at 298.15 K. The melting points were measured by DSC and are listed in Table 1. They were dissolved in 1mM excess aqueous solution of sodium hydroxide. Auramine (guaranteed reagent, Kanto Chemical Co.) was used as a fluorescence probe for determination of critical micelle concentration (cmc). The concentration of the probe molecule was 1×10^{-5} M.

Solubility

The solubility of *N*-hexadecanoyl amino acid was measured by HPLC (Japan Optics, BIP-1). After dissolving the *N*-hexadecanoyl amino acids in an aqueous solution of 0.4 M NaCl, the solutions were kept at 2 ˚C to deposit the solid Na *N*-hexadecanoyl amino acid salts. The addition of NaCl was necessary in order to raise the KT above 0 °C for almost all surfactants. The concentration of all the solutions prepared was ca. 0.1

mM. After the samples reached equilibrium in a thermostat at a given temperature, the supernatant solution was pipetted by syringe equipped with a disc filter (pore size 0.4μm). A reversed phase chromatography column (Tosoh co. TSKgel ODS-120A) and an UV-VIS monitor (Tosoh co. model UV-8000) were used as a packed column and a detector, respectively. The eluate was a mixed solution of methanol (80%) and 30mM aqueous solution of phosphoric acid (20%).

DSC

Differential scanning calorimetry (DSC) experiments were made by using a DSC7 (Perkin-Elmer) thermal analyzer. A sample solution was prepared in the same way as for the solubility measurements, and was sealed in a Large Volume Capsule (Perkin-Elmer) using an O-ring sealed 60 μl stainless steel container. The experiments were done on the solutions in the concentration range 5 to 20 mM using about 50 mg of the samples. After the samples were kept at 0 °C for 5 hours, they were heated at a rate of 0.5 K/min. At least four runs were performed each system.

Cmc

Fluorescence measurements were carried out on a Hitachi fluorescence spectrophotometer F-2000 for determination of cmc values of *N*-acyl amino acid surfactants. Excitation and emission wavelengths were 410 and 470 nm, respectively. The ratio of the fluorescence intensity in an aqueous solution containing no surfactant (I_0) against that for a surfactant solution (I) was used as indication of microviscosity and was measured as a function of concentration of surfactant and temperature.

Results

Solubility

Figure 2 shows the logarithm of the solubility of *N*-hexadecanoyl amino acid sodium salts obtained by HPLC as a function of temperature. For C16-DL-Ile, its solubility could not be determined because its KT was below 0 °C. From Figure 2 it can be seen that the solubility rises abruptly at a particular temperature in all systems. The temperatures correspond to the KT and these values are summarized in Table 2. The order of KT was C16-Ile < -Leu < -Val < -Phe < -Ala, which increased with decreasing size of residue except for C16-Phe. For the C16-Ala and C16-Phe systems, the KT of the DL form was higher than that of the L form. Conversely, for the C16-Val, C16-Leu, and C16-Ile systems the KT of the DL form was lower than that of the L form. Furthermore the solubility of C16-Phe below the KT was smaller one order of magnitude compared with the other systems, and its temperature dependence was much larger. This means that enthalpy of solution of C16-Phe is substantial as described in the next section.

DSC

The thermograms of a 10mM aqueous solution of Na *N*-hexadecanoyl amino acid surfactants in the presence of the solid deposit are shown in Fig. 3. It can be seen that an endothermic peak accompanies the dissolution of the surfactant around the KT. In this measurement, KT could be defined as the temperature corresponding to the onset of the peak and these values are shown in Table 2. The KT values determined by this method gave a

similar result to those obtained from the solubility measurements; C16-Leu < -Val < -Phe < -L-Ala < -DL-Ala ≈ -Gly. The enthalpy of solution was calculated from the peak area and is shown in Table 2. Except for C16-Gly and C16-Phe, enthalpy decreased with increasing size of the amino acid residue. When the KT of the DL-form is higher than that of the L-form, the enthalpy of the DL-form is correspondingly greater than that of the L-form. The enthalpy of solution of C16-Phe is surprisingly large compared to the others.

Cmc

Figure 4 shows a dependence of fluorescence intensity ratio (I/I_0) on concentration for several amino acid surfactants. The cmc was determined as the concentration at which the fluorescence intensity increases sharply. The cmc determined by this method is in good agreement with those obtained using other techniques, such as the surface tension method [22]. The results are shown in Fig. 5. With the exception of C16-Ala, the order of cmc reflects the magnitude of hydrophobicity of the amino acid residue (i.e. C16-Phe < -Ile < -Leu < -Val). It was confirmed that the concentration at the KT was equivalent to the cmc. Contrary to the melting point and KT, the difference in cmc between the L- and DL-form of amino acid surfactants was not obvious. We interpret this result as meaning the optical isomer was not developed in a micelle where surfactants were relatively loosely assembled compared with the solid state.

Discussion

Krafft temperature

We have shown that the KT of *N*-hexadecanoyl amino acid surfactants increased with decreasing the size of the hydrophobic residue of amino acid except for the case of phenylalanine. This suggests that the increase in size of the hydrophobic residue makes the molecular packing of surfactant loosen thereby causing the KT of surfactant to decrease. A comparison of the KT for C16-Leu and C16-Ile, indicates the molecular packing of surfactant becomes looser when the branch point of the residue is situated nearer to the main chain. Since both the solubility and the cmc of C16-Phe was the smallest, we conclude that this was the most hydrophobic surfactant in this study. Furthermore the aromatic ring of phenylalanine, is large and bulky compared to the other amino acid residues. The KT of C16-Phe, however, is relatively high and deviates from the series mentioned above. Rather than causing steric hindrance, access between the benzyl groups leads to a favorable interaction in the solid state, possibly stabilized by π-π or CH-π interactions between the aromatic rings [24].

The chiral effect of the amino acid can be divided into two types. Firstly where the KT of the DL-form is higher than that of the L-form (C16-Ala and -Phe), and secondly where the opposite is the case (C16-Val, -Leu, and -Ile). In the former case, the DL-form of the surfactant is obviously a racemic compound, while it seems to be a racemic mixture in the latter case. The KT of C16-DL-Ala is almost identical to that of C16-Gly. It is reasonable to suppose that C16-Gly, which has the smallest residue, can be oriented in the solid state most efficiently. This result suggests that a formation of the molecular pair between the L-form and the D-form of C16-Ala is very effective at enhancing the molecular packing in the solid state as is the case for C16-Gly. This is a question to be considered later. A large residue may prevent the molecular packing, thus

the DL-forms of C16-Val, -Leu, and -Ile have a lower KT than the L-forms. From the viewpoint of residue size, phenylalanine, which contains an aromatic ring, can be considered an exceptional case. As mentioned above, the interaction between the benzyl groups is favorable and is enhanced by a combination of the L- and D-forms. Note that the KT of C16-L-Val is higher than that of C16-DL-Val contrary to the melting point. This may suggest that the nature of the counter ion affects the chiral discrimination.

Enthalpy of solution

The enthalpy of solution Δh_{sol} obtained in this study corresponds to the difference between the enthalpy of surfactant in the micellar state h(micelle) and that in the solid state h(solid).

$$\Delta h_{sol} = h(\text{micelle}) - h(\text{solid}) \qquad [1]$$

As we have mentioned in the previous section, the increase in size of the hydrophobic residue causes looser molecular packing in the solid state and weaker hydration of surfactant in the micellar state. The effect raises the values of h(solid) and h(micelle). Therefore the difference of Δh_{sol} among C16-Ala, C16-Val, and C16-Leu is principally attributable to h(solid), while that between C16-Ala and C16-Gly is caused by the variance of h(micelle). The Δh_{sol} value of C16-Phe was greatest of all in this study. This is because C16-Phe has both the largest h(micelle), which is due to the contact of the hydrophobic benzyl group with water molecules in the micellar state, and the smallest h(solid), which is due to the interaction between the benzyl groups in the solid state.

The chiral effect of the amino acid on the enthalpy of solution followed two trends. For C16-Ala and C16-Phe, the Δh_{sol} of the DL-form

was higher than that of the L-form, whereas the converse was true for C16-Val and C16-Leu. This classification is equivalent to that for the KT. This fact supports the above conclusion that C16-DL-Ala and C16-DL-Phe form racemic compounds while C16-DL-Val and C16-DL-Leu are just mixtures. Since the racemic effect was very small in a micelle [2], the enthalpy of formation of racemic compound Δh_{rac} could be evaluated by subtracting the Δh_{sol} value of the DL-form from that of the L-form under the condition that the temperature dependence of enthalpy might be ignored.

$$\begin{aligned}\Delta h_{\mathrm{rac}} &= h_{\mathrm{DL}}(\mathrm{solid}) - \frac{1}{2}\left[h_{\mathrm{L}}(\mathrm{solid}) + h_{\mathrm{D}}(\mathrm{solid})\right] \\ &= h_{\mathrm{DL}}(\mathrm{solid}) - h_{\mathrm{L}}(\mathrm{solid}) = \Delta h_{\mathrm{sol,\ L}} - \Delta h_{\mathrm{sol,DL}}\end{aligned} \qquad [2]$$

The values obtained for Δh_{rac} of C16-Ala and C16-Phe were –13 kJ mol^{-1} and –61 kJ mol^{-1}, respectively. These values are much larger than the interaction energies between either methyl or benzyl groups and correspond to the energy of hydrogen bonding. The combination of the L- and D-forms of C16-Ala or C16-Phe enhances the contribution of hydrogen bonding between adjacent peptide groups of the surfactant. This is especially significant for C16-Phe where the value of Δh_{rac} is very large. In addition to the increased hydrogen bonding between the peptide groups and hydrophobic interactions between the benzyl groups, contact between the acyl moiety is also enhanced for the C16-DL-Phe system.

Calculated structure of Na *N*-acetyl alaninate dimer

We have applied *ab initio* calculation to clarify the difference between the L- and DL-form of Na C16-Ala. The dimer of sodium *N*-acetyl alaninate (see Fig. 6(a)) was employed as a model compound for

simplification of calculation in this study. The dimerization energy and the optimized geometry were calculated by using the restricted Hartree-Fock (RHF) procedure with the 6-31 + G* basis set. All calculations were performed using Gaussian 98 [25].

Obtained geometries of L-L and D-L dimers are shown in Fig. 6(b). Each dimer is built by coordination of two carboxylates to two sodium ions simultaneously. The top view of the two structures seem to be similar to each other. Indeed the calculated dimerization energies were –93.856 and –93.869 kJ mol^{-1} for the L-L and D-L dimers, respectively. However, the difference is clear from the side view of the structures in Fig. 6(c). In the D-L dimer, each alanine residue is situated in the *trans* position through the bonding between carboxylates, while in the *gauche* position for the L-L dimer. Although this explains the small difference in the dimerization energies between the L-L and D-L dimers obtained by *ab initio* calculations, it does not explain the difference in Δh_{rac} obtained by DSC measurements. Of course in the experimental system, the interaction between not only the dimers but also the neighboring molecules are investigated. In this case, one of the most significant interactions is the hydrogen bonding between adjacent peptide groups. When this was taken into consideration, it was found that the dimers could interact with the two adjacent molecules at the two hydrogen bond lines (Fig 6[b] and Fig. 6[c]). It should be noted that one line is parallel to the other in the D-L dimer, whereas the two lines intersect each other in the L-L dimer (Fig. 6[c]). This suggests that the DL form of Na *N*-acyl alaninate can create a sheet structure stabilized by hydrogen bonds between the peptide groups more effectively than the L-form. Therefore, Na *N*-acyl DL-alaninate becomes a racemic compound in the solid state. This could explain why Na *N*-acyl

DL-valinate and DL-leucinate are less stable than their L-form counterparts, since the larger hydrophobic residues may hinder the stacking in the sheet-like structure. Conversely, in the case of Na *N*-acyl DL-phenylalaninate, contact between the benzyl groups in the sheet structure is an advantageous factor and results in the racemic compound.

Conclusions

The Krafft temperature of *N*-hexadecanoyl amino acid surfactant increased with decreasing size of the amino acid residue of except for the case of phenylalanine, the enthalpy of solution was increased with decreasing size of the amino acid residue except for the cases of glycine and phenylalanine. Experimental results showed that the D-L interaction was superior to the L-L interaction in the solid state of *N*-hexadecanoyl amino acid surfactant salt for both the alanine and phenylalanine systems, while the L-L interaction was advantageous for both the valine and leucine systems. It was suggested that both the peptide-peptide hydrogen bonding and the steric hindrance of the amino acid residue govern the chiral effect.

References

1. Takehara M (1984) Hyomen(in Japanese) 35: 459
2. Miyagishi S, Nishida M (1978) J Colloid Interface Sci 65: 380
3. Miyagishi S, Kurimoto H, Asakawa T (1995) Langmuir 11: 2951
4. Miyagishi S, Akasofu W, Hashimoto T, Asakawa T (1996) J Colloid Interface Sci 184: 527
5. Miyagishi S. Suzuki H. Asakawa T (1996) Langmuir 12: 2900
6. Etori H, Hirata H, Yamada Y, Okabayashi H, Furusaka M (1997) Colloid Polym Sci 275: 263

7. Ishida M, Takai M, Okabayashi H, Masuda H, Furusaka M, O'Connor C J (2001) Colloid Polym Sci 279: 1034
8. Miyagishi S, Takeuchi N, Asakawa T, Inoh M (2001) Colloids Surfaces A 197: 125
9. Miyagishi S, Matsuura S, Murata K, Asakawa T, Nishida M (1985) Bull Chem Soc Jpn 58: 1019
10. Miyagishi S, Matsuura S, Asakawa T, Nishida M. (1986) Bull Chem Soc Jpn 59: 557
11. Harvry N G, Mirajovsky D, Rose P L, Verbiar R, Arnett R M (1989) J Am Chem Soc 111: 1115
12. Stine K J, Uang J Y -J, Dingman S D (1993) Langmuir 9: 2112
13. Gericke A, Hühnerfuss H (1994) Langmuir 10: 3782
14. Parazak D P, Uang J Y -J, Turner B, Stine K J (1994) Langmuir 10: 3787
15. Hoffmann F, Hühnerfuss H, Stine K J (1998) Langmuir 14: 4525
16. Shinitzky M, Haimovitz R (1993) J Am Chem Soc 115: 12545
17. Wang J, Waner I M (1995) J Chromatogr A 711: 297
18. Rugutt J K, Billot E, Waner I M (2000) Langmuir 16: 3022
19. Yarabe H H, Rugutt J K, McCarroll M E, Waner I M (2000) Electrophoresis 21: 2025
20. Cohen S A, Paulus A, Karger B L (1987) Chromatographia 24: 15
21. de Bruin T J M, Marcelis A T M, Zuilhof H, Sudhölter E J R (2000) J Phys Chem B 16: 8270
22. Miyagishi S, Kutimoto H, Ishihara Y, Asakawa T (1994) Bull Chem Soc Jpn 67: 2398
23. Ohta A et al unpublished result
24. Umezawa Y, Tsuboyama S, Honda K, Uzawa J, Nishio M (1998) Bull Chem Soc Jpn 71: 1207
25. Frisch M J, Trucks G W, Schlegel H B, Scuseria G E, Robb M A, Cheeseman J R, Zakrzewski V G, Montgomery J A, Stratmann R E, Burant J C, Dapprich S, Millam J M, Daniels A D, Kudin K N, Strain M C, Farkas O, Tomasi J, Barone V, Cossi M, Cammi R, Mennucci

B, Pomelli C, Adamo C, Clifford S, Ochterski J, Petersson G A, Ayala P Y, Cui Q, Morokuma K, Malick D K, Rabuck A D, Raghavachari K, Foresman J B, Cioslowski J, Ortiz J V, Stefanov B B, Liu G, Liashenko A, Piskorz P, Komaromi I, Gomperts R, Martin R L, Fox D J, Keith T, Al-Laham M A, Peng C Y, Nanayakkara A, Gonzalez C, Challacombe M, Gill P M W, Johnson B G, Chen W, Wong M W, Andres J L, Head-Gordon M, Replogle E S, Pople J A (1998) Gaussian 98 (Revision A.9). Gaussian Inc, Pittsburgh, PA

Figure Captions

Fig. 1 Chemical structure of *N*-hexadecanoyl amino acid.

Fig. 2 Temperature dependence of solubility of Na C16-amino acid salt in aqueous 1mM NaOH and 0.4M NaCl. (full-circle) L-form, (open-circle) DL-form.

Fig. 3 Thermograms of the 10mM of the aqueous solutions of Na C16-amino acid salt. (solid line) L-form, (dotted line) DL-form.

Fig. 4 Dependence of a fluorescence intensity ratio (I/I_0) on concentration for several amino acid surfactants in aqueous 1mM NaOH and 0.4M NaCl. (1) C16-Val at 308.15 K, (2) C16-Leu at 308.15 K, (3) C16-Ile at 308.15 K, (4) C16-Ala at 318.15 K.

Fig. 5 Critical micelle concentration vs temperature curves. (1) C16-Val, (2) C16-Leu, (3) C16-Ile, (4) C16-Phe*, (5) C16-Ala. (The lines are guide for eyes.) * by surface tension measurement [23]

Fig. 6 (a) Chemical structure of dimer of sodium *N*-acetyl alaninate, (b) Top view of optimized dimer geometries, (c) Side view of optimized dimer geometries.

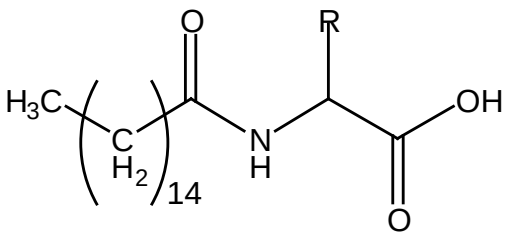

amino acid	residue (-R)
Gly	-H
Ala	$-CH_3$
Val	$-CH(CH_3)_2$
Leu	$-CH_2CH(CH_3)_2$
Ile	$-CH(CH_3)CH_2CH_3$
Phe	$-CH_2C_6H_5$

Fig. 1 Chemical structure of *N*-hexadecanoyl amino acid.

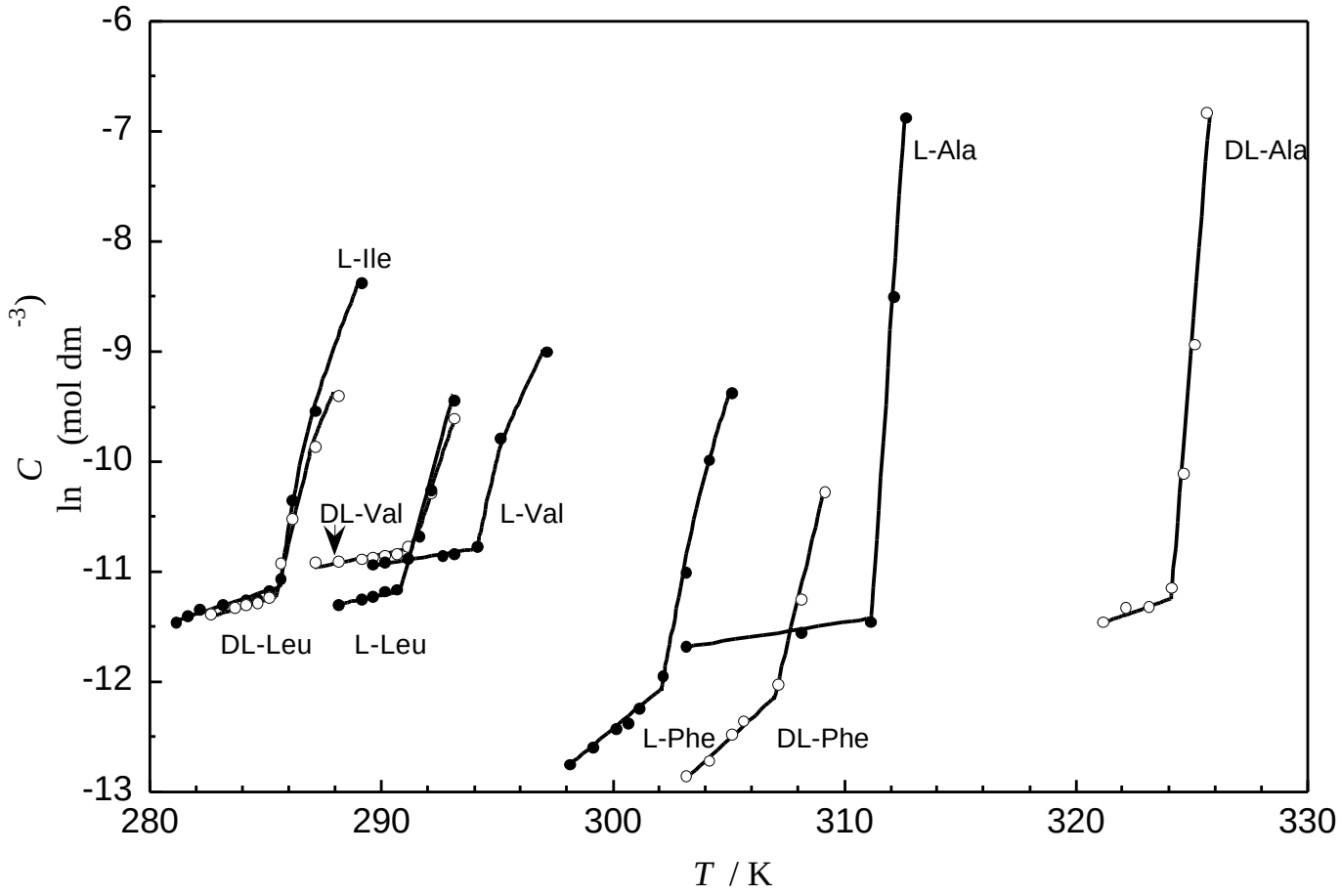

Fig. 2 Temperature dependence of solubility of Na C16-amino acid salt in aqueous 1mM NaOH and 0.4M NaCl. (full-circle) L-form, (open-circle) DL-form.

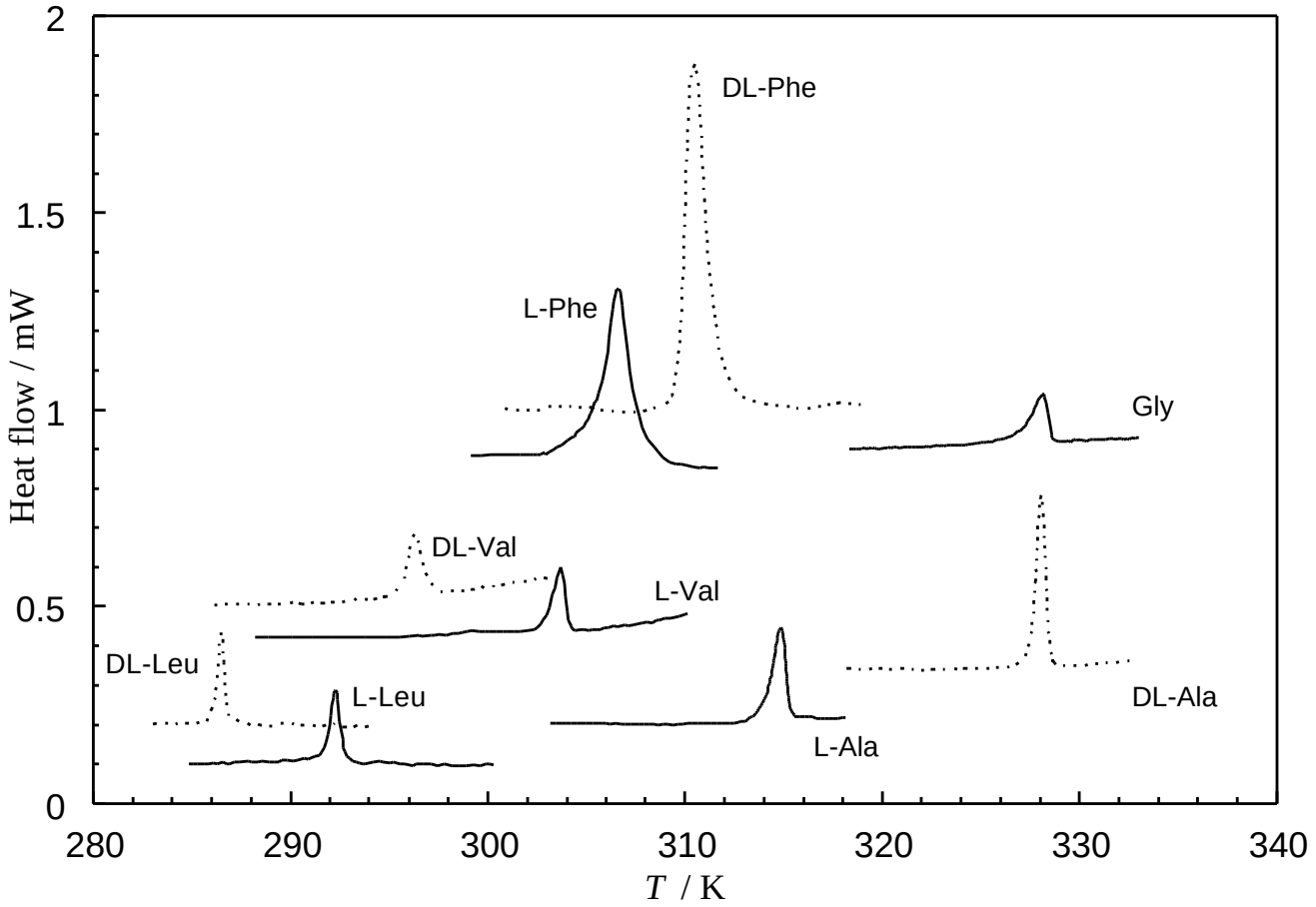

Fig. 3 Thermograms of the 10mM of the aqueous solutions of Na C16-amino acid salt. (solid line) L-form, (dotted line) DL-form.

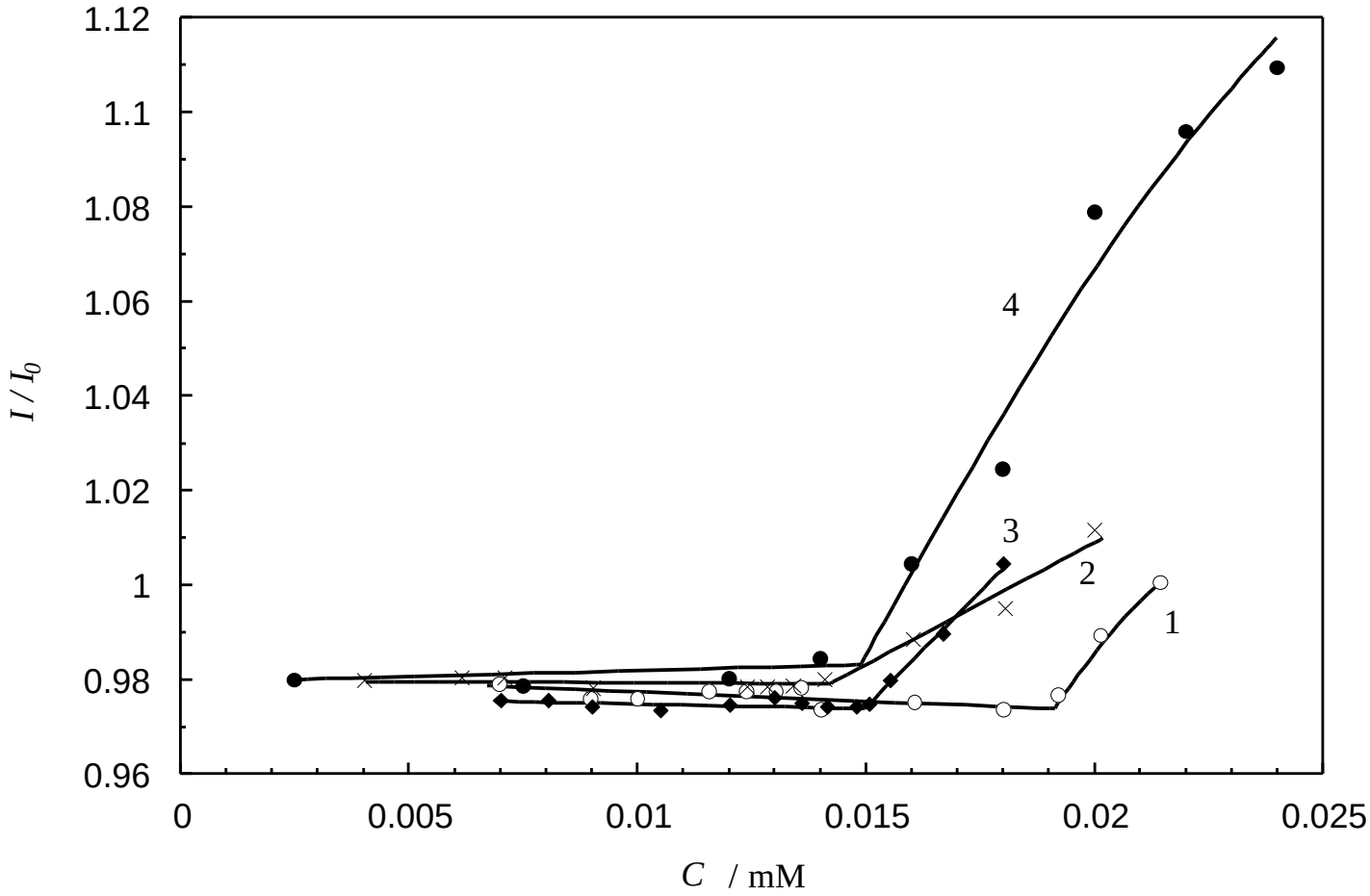

Fig. 4 Dependence of a fluorescence intensity ratio (I/I_0) on concentration for several amino acid surfactants in aqueous 1mM NaOH and 0.4M NaCl. (1) C16-Val at 308.15 K, (2) C16-Leu at 308.15 K, (3) C16-Ile at 308.15 K, (4) C16-Ala at 318.15 K.

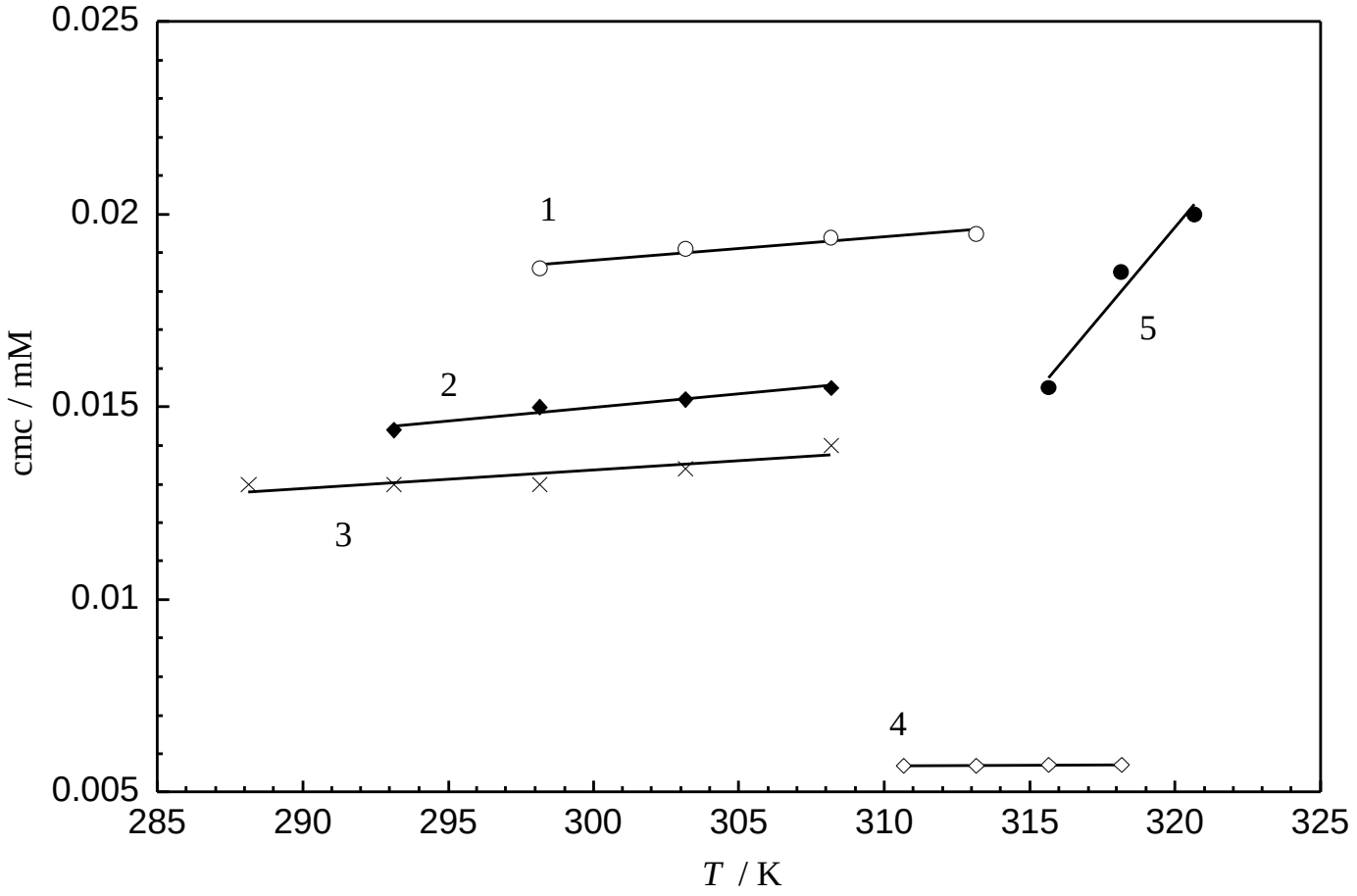

Fig. 5 Critical micelle concentration vs temperature curves. (1) C16-Val, (2) C16-Leu, (3) C16-Ile, (4) C16-Phe*, (5) C16-Ala. (The lines are guide for eyes.) * by surface tension measurement [23]

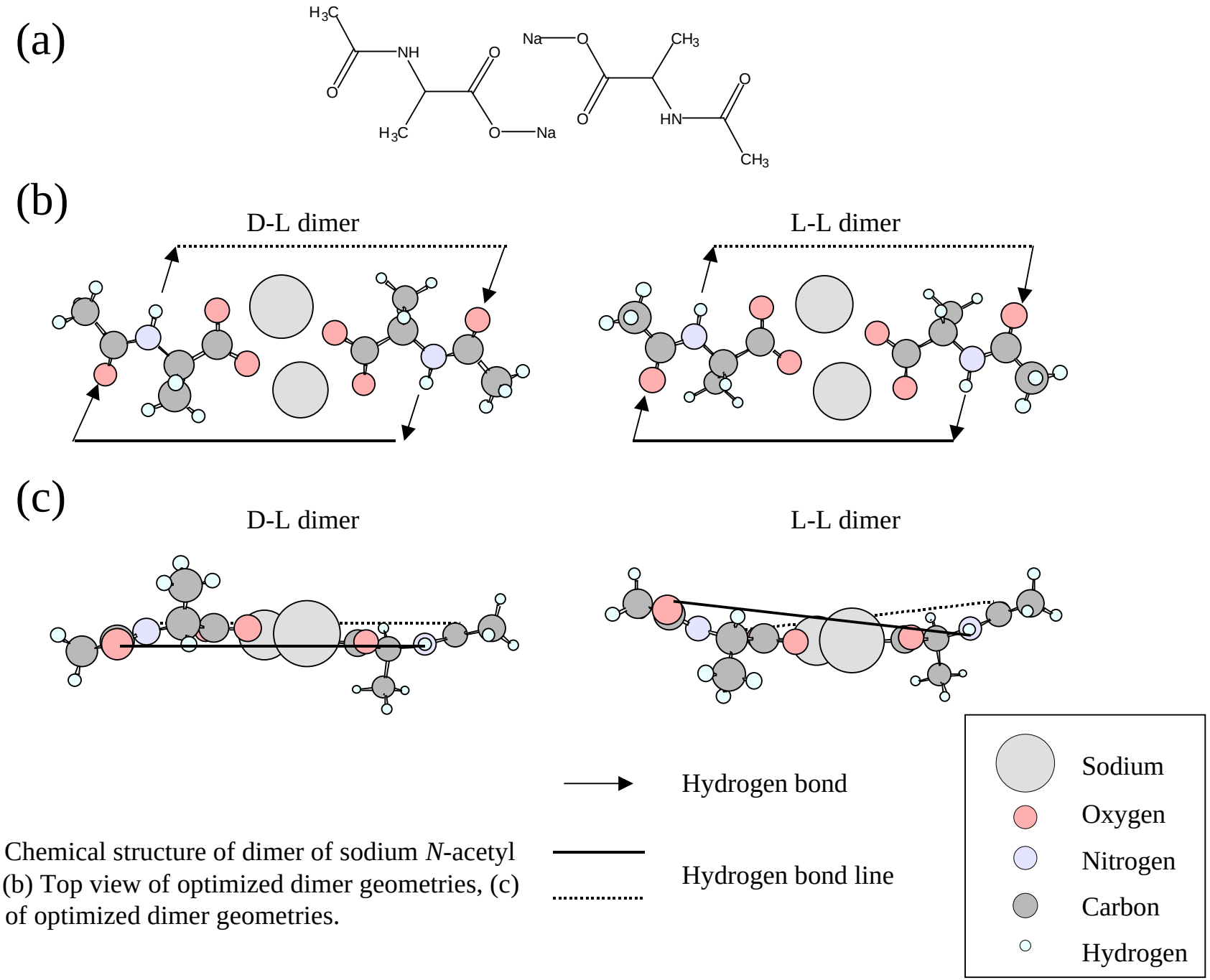

Fig. 6 (a) Chemical structure of dimer of sodium *N*-acetyl alaninate, (b) Top view of optimized dimer geometries, (c) Side view of optimized dimer geometries.